SUPPLEMENTARY INFORMATION

SUPPLEMENTARY FIGURE

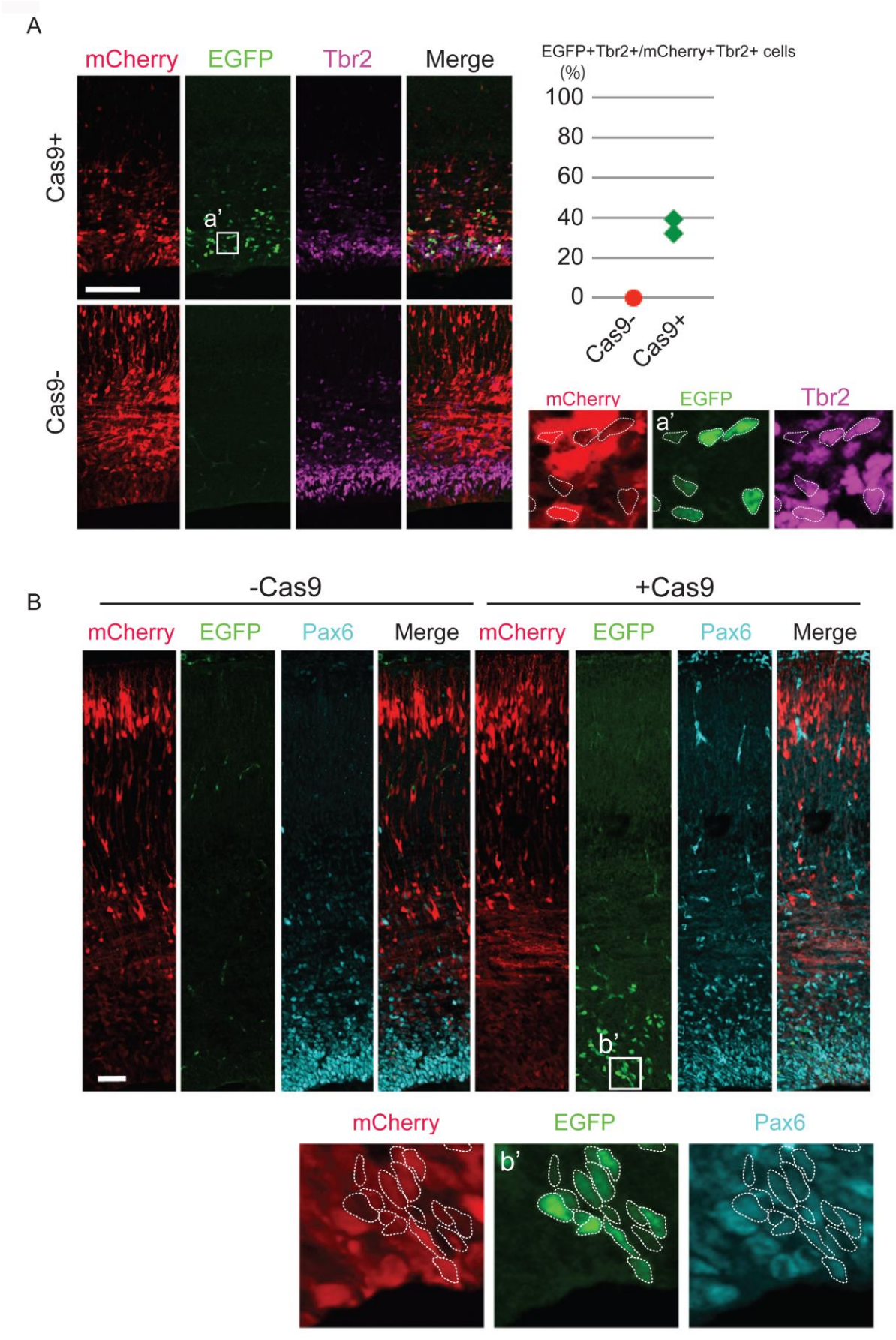

Fig. S1

(A) EGFP *de novo* KI to C-terminus of the *Tbr2* locus. *In utero* electroporation was performed with the pCAX-Cas9, the pCAG-mCherry-gRNA and the targeting vector against Tbr2 at E13.5 followed by fixation at E17.5. The pCAG-mCherry-gRNA and the targeting vector without pCAX-Cas9 were electroporated as a negative control. EGFP positive cells were observed only in the samples that have been electroporated with Cas9. All EGFP-positive cells were co-immunostained with the anti-Tbr2 antibody (a', alined white). The distribution of KI efficiency (EGFP / Tbr2 double positive cells out of mCherry / Tbr2 double positive cells). The percentages were 0% for Cas9- negative control (n=2) and 39.1% and 32.1% for Cas9+ samples (n=2). We note that a defective migration was observed for cortical neurons in the KI sample even for those without KI (mCherry-positive, GFP-negative). This defect may be off-target effects specific for the gRNA used in this experiment. (B) EGFP *de novo* KI to C-terminus of *Pax6* locus. pCAX-Cas9, the pCAG-mCherry, gRNA expression vector and the Pax6 targeting vector was electroporated at E13.5 then fixed at f E17.5. Cas9- negative control showed no EGFP signals but few blood vessel backgrounds. EGFP positive cells were observed in the samples that have been electroporated with Cas9, all EGFP-positive cells were co-immunostained with the anti-Tbr2 antibody (b', aligned white). Scale bar: (A) 100 μm, (B) 40 μm.

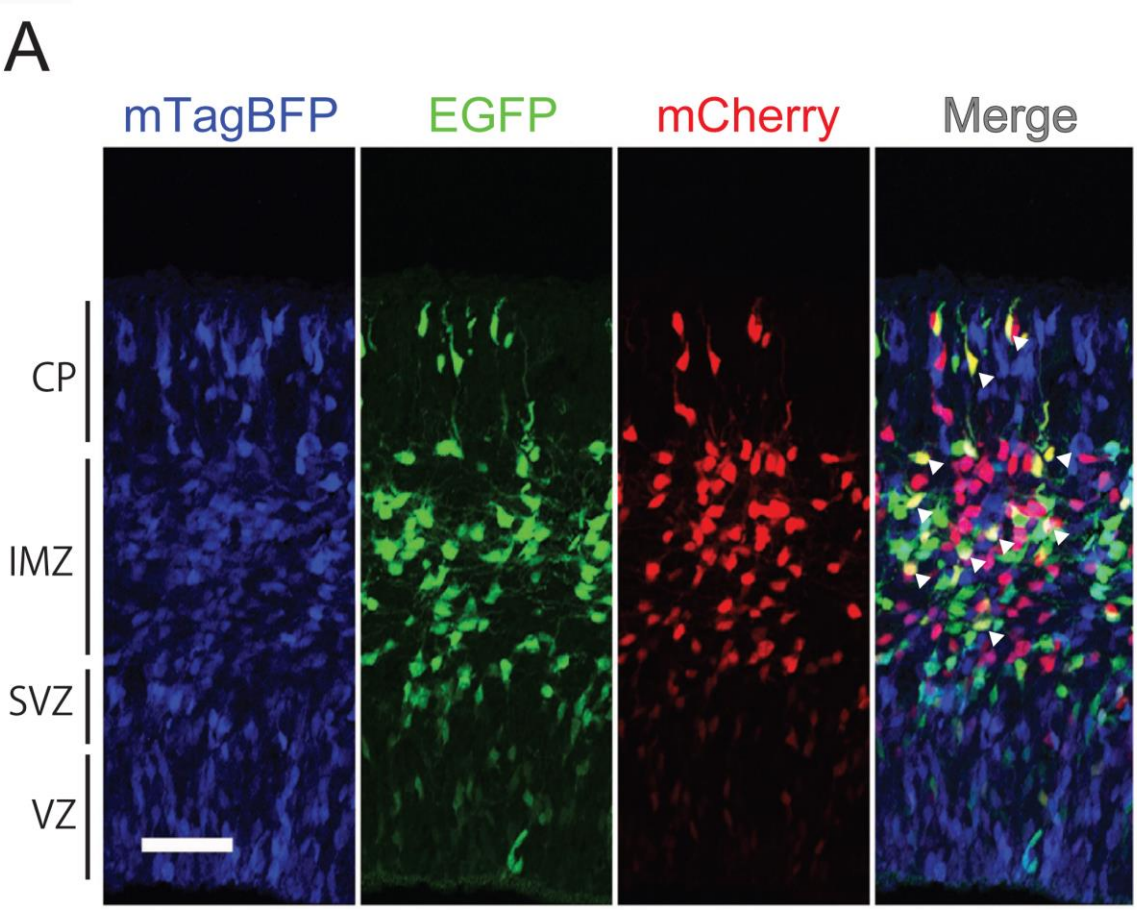

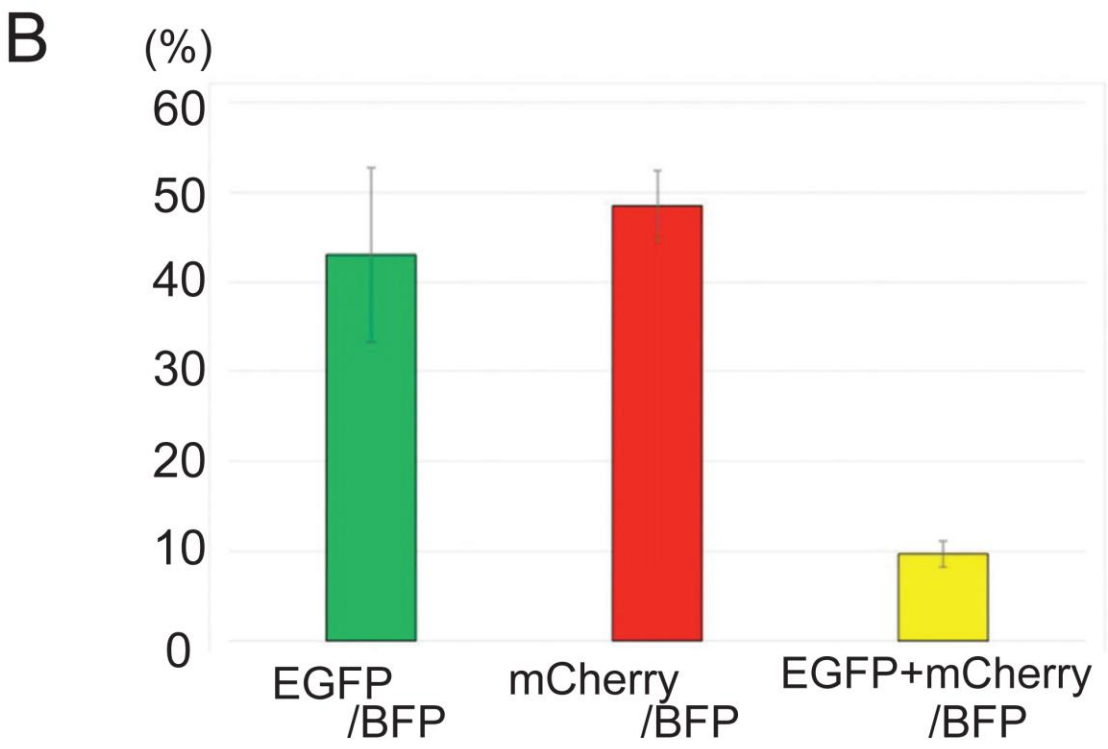

Fig. S2

Homozygous *de novo* KI via *in utero* electroporation for 2 days. (A) Embryos were electroporated at E12.5 and fixed at E14.5. EGFP/mCherry-double positive cells were observed, suggesting that both alleles of the *Tubb3* gene were knocked in by the donor EGFP and mCherry (arrowheads). (B) Quantitative measurement of the EGFP-positive, mCherry-positive and EGFP/mCherry-double positive cells out of the electroporated cells in the region outside the ventricular zone. The percentage was 43.02±9.72% for EGFP-positive cells, 48.44±3.96% for mCherry-positive cells, and 9.68±1.46% for EGFP/mCherry double-positive cells (n= 6 embryos). Error bars indicate SD.

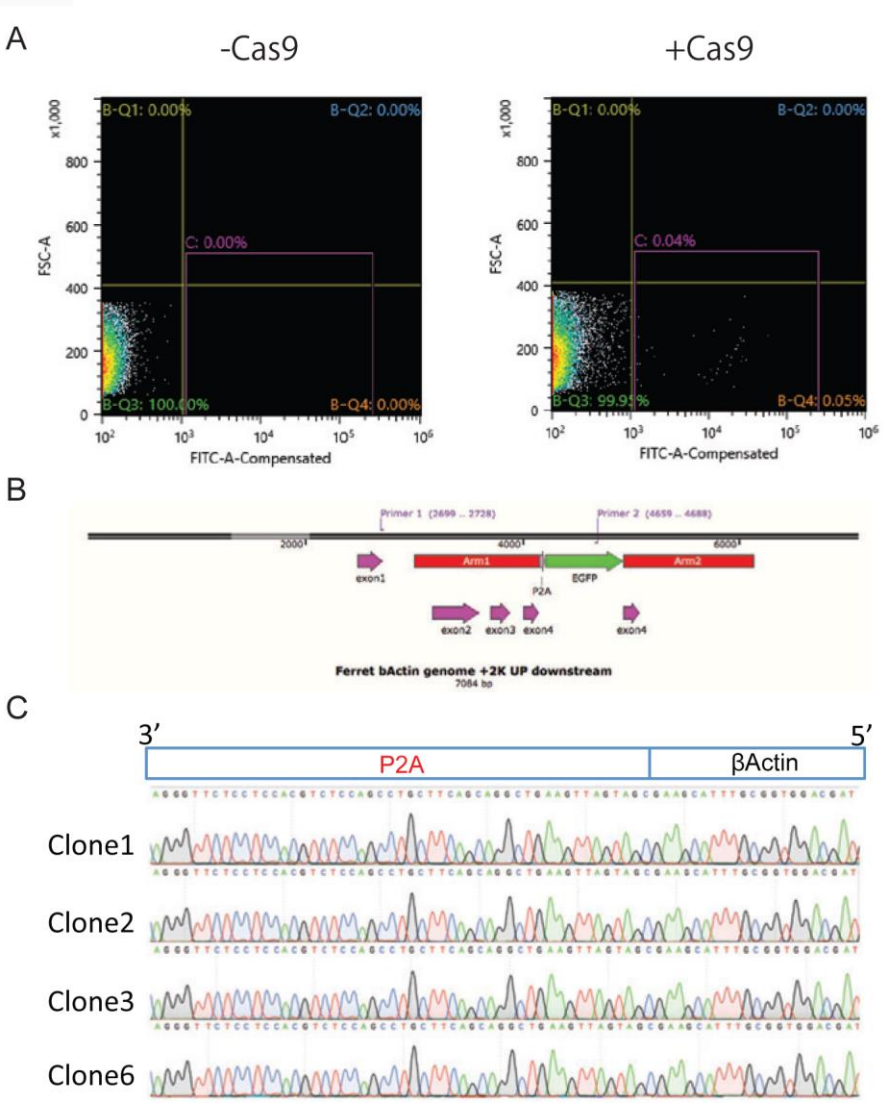

Fig. S3

Sequence confirmation of *de novo* KI in ferret neural progenitors. (A) FACS for EGFP-positive cells. Embryo brains were dissected and dissociated, and then EGFP-positive cells were sorted through gate-C. (B) Schematic presentation of the ferret *ACTB* locus. The forward primer for genome amplification was constructed out of a homology arm, which can amplify the joint part of the genome and the donor DNA. (C) Sequences of individual clones. Six individual clones were sequenced. Five clones contain a genomic amplicon. All sequences show the correct joint between the Actb C-terminal sequence and the donor. Four examples are shown.

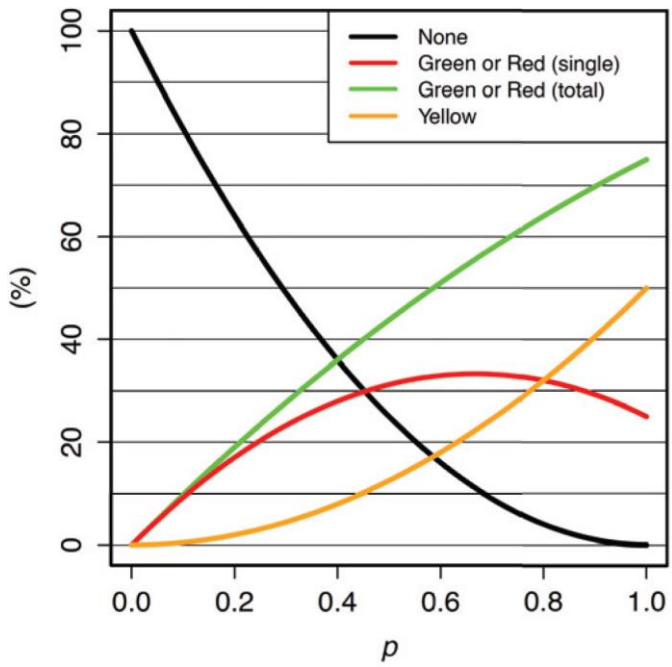

Fig. S4

Theoretical frequencies of fluorescent colors as functions of knock-in probability. Black line indicates frequency of cells without KI. Red line indicates frequency of cells only with a single fluorescent color. Yellow line indicates frequency of cells with both fluorescent colors. Green line indicates frequency of cells with a fluorescent color irrespectively of another color expression.

SUPPLEMENTARY MATERIALS AND METHODS

in utero electroporation

Mouse *in utero* electroporation was performed as described previously (Konno et al., 2008). Pregnant ICR mice were anesthetized by 650 µl IP injection of 10% Nembutal (Sumitomo Dainippon Pharma, Oasaka Japan). The mixture of pCAX-hCas9 (0.5µg/µl), the gRNA vector (0.5 µg/µl) and the targeting vector (0.5 µg/µl) were injected into the brain hemisphere, containing the 0.005% Fast Green FCF (Wako Pure Chemical Industries, Osaka Japan). Embryos were tweezed by paddles of the tweezer electrodes (CUY21 electroporator, NEPA GENE, Ichikawa Japan), then subjected to 5×50 ms/ 35 V (for E12.5, 13.5) or 45 V (for E15.5) electric pulses.

Immunohistochemistry

Mouse brains were fixed in 1% paraformaldehyde in phosphate buffer, pH 7.4, at 4°C for 2 h or over night, followed by cryoprotection in 25% sucrose overnight at 4°C. Fixed brains were embedded in O.C.T. compound (Sakura Finetek, Tokyo, Japan) and sectioned at 12 µm thickness by cryostat. Brain sections were treated with HistVT one antigen retrieval solution (Nacalai tesque, Kyoto Japan) for 20min at 70°C, washed three times with PBST (PBS with 0.1% Tween-20), and then treated with the blocking buffer (2% donkey serum and 0.2% Triton X-100 in PBS, pH 7.4) for 1 h at room temperature, followed by the incubation with primary antibodies diluted in the same buffer overnight at 4°C. Sections were washed three times in PBST and treated with secondary antibodies for 1 h at room temperature. The stained sections were mounted with PermaFluor mounting medium (Thermo Fisher Scientific Waltham US). Ferret brains were fixed in 1% paraformaldehyde in phosphate buffer, pH 7.4, at 4°C for two overnights, washed with PBS overnight at 4°C, and embedded in 4% low melting point agarose (UltraPure LMP agarose, Thermo Fisher Scientific Waltham US). Embedded brains were sliced at 200 µm thickness by vibratome (LinerSlicer, DOSAKA EM, Kyoto Japan). Brain slices were washed three times with PBST, treated with the blocking buffer for 1 h at room temperature, and incubated with primary antibodies for 4 overnights at 4°C under shaking. Brain slices were washed three times in PBST and treated with secondary antibodies for 4 overnights at 4°C under shaking. After being washed, the brain slices were mounted with CUBIC solution 2 to be transparent (Susaki et al., 2014). Stained sections and slices were observed with a confocal microscope (FV1000, Olympus Tokyo Japan; LSM510, Zeiss, Jena Germany, and CSU-W1 Yokogawa Electric, Tokyo Japan). The antibodies

used in this study are listed below. Primary antibodies; Mouse anti-α-tubulin (Sigma T9026, 1/100), Mouse anti-Pax6 (DSHB #AB528427, 1/500), Rat anti-RFP (Chromotek #5F8, 1/1000), Chick anti-EGFP (Aves #GFP-1020, 1/1000), Rabbit anti-tRFP DL405 conjugated (Evrogen #AB233, 1/100, which recognizes mTagBFP), Rabbit anti-Eomes (Abcam #ab23345, 1/1000), Rat anti-mouse Eomes eFluor 660 conjugated (eBioscience #50-4875-82, 1/1000). Secondary antibodies; Donkey anti-Mouse-Cy5 (Jackson #715-175-151, 1/500), Donkey anti-Rat-Cy3 (Jackson #712-165-150, 1/500), Donkey anti-Rabbit-AMCA (Jackson #711-155-152, 1/500), Donkey anti-Chicken-Alexa Fluor 488 (Jackson #703-545-155, 1/500).

Mathematical model of double knock-in efficiency

Assume that knock-in and in/del mutation at a chromosome locus induced by a single

DSB occur at certain probability p_{ki} $(0 \leq p_{ki} \leq 1)$ and p_m $(0 \leq p_m \leq 1,\ p_{ki} + p_m \leq 1)$, respectively. If DSB was repaired without KI or mutation, a DSB is generated again. After n $(n = 1, 2, \dots)$ times of DSB induction, eventual KI frequency designated as p is given by

$$p = \sum_{i=1}^{n} (1 - p_{ki} - p_m)^{i-1} \cdot p_{ki},$$

which can be transformed as

$$p = \frac{p_{ki} - (1 - p_{ki} - p_m)^n \cdot p_{ki}}{p_{ki} + p_m}.$$

Especially in case that n is large enough,

$$p \approx \frac{p_{ki}}{p_{ki} + p_m}.$$

Consider the eventual knock-in efficiency p as probability of KI at individual chromosomes. Given that knock-in at each chromosome occurs independently, number of KI chromosome(s) per cells follows a binomial distribution. Because DSB occurs during the S phase and G2 phase, it is reasonable to assume 4 chromosomes are susceptible of DSB for a single cell prior to cell division. Thus, the expected frequencies of KI chromosome(s) number per cells are given by followings:

No knock-in, $(1 - p)^4$.

1 knock-in, $4p(1 - p)^3$.

2 knock-in, $6p^2(1 - p)^2$.

3 knock-in, $4p^3(1 - p)$.

4 knock-in, p^4.

After recombination finished, chromosomes are segregated to two daughters. Given that the insertion of green or red fluorescent genes occurs by chance, segregation of fluorescent colors to daughter cells are considered as follows.

Knock-in number		0	1	2	3	4	Frequency
Probability		$(1-p)^4$	$4p(1-p)^3$	$6p^2(1-p)^2$	$4p^3(1-p)$	p^4	
Weight of daughter cell color	No knock-in	1	$\frac{1}{2}$	$\frac{1}{6}$	0	0	$(1-p)^2$
	Hetero Green	0	$\frac{1}{4}$	$\frac{1}{3}$	$\frac{1}{4}$	0	$p(1-p)$
	Hetero Red	0	$\frac{1}{4}$	$\frac{1}{3}$	$\frac{1}{4}$	0	$p(1-p)$
	Homo Green	0	0	$\frac{1}{24}$	$\frac{1}{8}$	$\frac{1}{4}$	$\frac{1}{4}p^2$
	Homo Red	0	0	$\frac{1}{24}$	$\frac{1}{8}$	$\frac{1}{4}$	$\frac{1}{4}p^2$
	Homo Yellow	0	0	$\frac{1}{12}$	$\frac{1}{4}$	$\frac{1}{2}$	$\frac{1}{2}p^2$
Total		1	1	1	1	1	1

From these probability values, frequencies of daughter cell colors are estimated as followings:

No KI,

$$f_{\text{none}} = (1-p)^4 + \frac{1}{2}\cdot 4p(1-p)^3 + \frac{1}{6}\cdot 6p^2(1-p)^2 = (1-p)^2.$$

Each hetero green and hetero red,

$$f_{\text{single.hetero}} = \frac{1}{4}\cdot 4p(1-p)^3 + \frac{1}{3}\cdot 6p^2(1-p)^2 + \frac{1}{4}\cdot 4p^3(1-p) = p(1-p).$$

Each homo green and homo red,

$$f_{\text{single.homo}} = \frac{1}{24}\cdot 6p^2(1-p)^2 + \frac{1}{8}\cdot 4p^3(1-p) + \frac{1}{4}\cdot p^4 = \frac{1}{4}p^2.$$

Homo yellow,

$$f_{\text{yellow}} = \frac{1}{12}\cdot 6p^2(1-p)^2 + \frac{1}{4}\cdot 4p^3(1-p) + \frac{1}{2}\cdot p^4 = \frac{1}{2}p^2.$$

Also, frequency of cells that have a single fluorescent color is given by

$$f_{\text{single}} = f_{\text{single.hetero}} + f_{\text{single.homo}} = p(1-p) + \frac{1}{4}p^2 = p - \frac{3}{4}p^2$$

and that of total green or red cells irrespectively of another color expression is given by

$$f_{\text{total}} = f_{\text{single}} + f_{\text{yellow}} = p - \frac{3}{4}p^2 + \frac{1}{2}p^2 = p - \frac{1}{4}p^2.$$

f_{none}, f_{single}, f_{total} and f_{yellow} as functions of p are shown in Figure S4.

SUPPLEMENTARY REFERENCE

Susaki, E. a., Tainaka, K., Perrin, D., Kishino, F., Tawara, T., Watanabe, T. M., Yokoyama, C., Onoe, H., Eguchi, M., Yamaguchi, S., et al. (2014). Whole-brain imaging with single-cell resolution using chemical cocktails and computational analysis. *Cell* **157**, 726–739.